Review

Dynamic Analysis of Shells

Charles R. Steele
Jason A. Tolomeo
Deborah E. Zetes
Division of Applied Mechanics
Stanford University
Stanford, CA 94305

Shell structures are indispensable in virtually every industry. However, in the design, analysis, fabrication, and maintenance of such structures, there are many pitfalls leading to various forms of disaster. The experience gained by engineers over some 200 years of disasters and brushes with disaster is expressed in the extensive archival literature, national codes, and procedural documentation found in larger companies. However, the advantage of the richness in the behavior of shells is that the way is always open for innovation. In this survey, we present a broad overview of the dynamic response of shell structures. The intention is to provide an understanding of the basic themes behind the detailed codes and stimulate, not restrict, positive innovation. Such understanding is also crucial for the correct computation of shell structures by any computer code. The physics dictates that the thin shell structure offers a challenge for analysis and computation. Shell response can be generally categorized by states of extension, inextensional bending, edge bending, and edge transverse shear. Simple estimates for the magnitudes of stress, deformation, and resonance in the extensional and inextensional states are provided by ring response. Several shell examples demonstrate the different states and combinations. For excitation frequency above the extensional resonance, such as in impact and acoustic excitation, a fine mesh is needed over the entire shell surface. For this range, modal and implicit methods are of limited value. The example of a sphere impacting a rigid surface shows that plastic unloading occurs continuously. Thus, there are no short cuts; the complete material behavior must be included.

INTRODUCTION

Although the shell is just a special case of continuum mechanics, there are several features that cause difficulty. These features are generally discussed in the vast literature on shells and shell structures. However, it is a formidable task, requiring literally years of diligent effort to decipher, assimilate, and use this information. Probably the majority of analysts who have responsibility for shell structures have neither the time nor the inclination to become such a specialist. Therefore, we assume only that the reader has familiarity with the concepts of dynamic response of a system with a finite number of degrees of freedom. We wish to extract the basic features of shell behavior, some of which are similar to the usual finite degree of freedom system, and some of which differ radically. The subject of shell stability is perhaps even more complex, but will not be touched upon in this article.

The difficulties associated with shell analysis from a computational viewpoint are indicated by a quote from MacNeal (1994):

> Curved shell elements include all of the features of two-dimensional elastic elements and plate bending elements, plus new complexities arising from the curved geometry. Shell elements are considered to be the most difficult of all elements and are the constant subject of advanced research.

An indication of the intrinsic difficulty in the analysis of shells is that the simplest linear, first ap-

Received March 2, 1995; Accepted April 4, 1995.
Shock and Vibration, Vol. 2, No. 5, pp. 413–426 (1995)

CCC 1070-9622/95/050413-14

proximation theory for shells was established to the satisfaction of most research workers only around 1960, beginning with Sanders (1959). In the field of finite element methods, no shell element with curvature in both directions has yet achieved such a consensus. On more than one occasion it has been mentioned that from a computational standpoint, general three-dimensional problems are easier than shells. Consequently, it is often the case that an analyst will abandon shell elements and use three-dimensional brick elments in layers through the shell thickness. At the opposite, analysts often approximate the shell with facets of flat-plate elements. The bricks greatly increase the number of elements required, and the replacement of a smooth surface with flat facets can greatly increase the error, particularly for smooth surface loading.

Nevertheless, substantial progress has been made with shell elements and is continuing to be made at a rapid rate. A number of computer codes can produce excellent results. Furthermore, the user preparation time, which not too long ago was measured in man-months for a shell structure of modest complexity, has been shortened to days if not hours, by advances in automated mesh generation and postprocessing. There are a number of publications that document the details of this advance, including Brebbia (1985), Hughes and Hinton (1986), Kardestuncer (1987), and Noor et al. (1989). Two of the many basic texts on the finite element method are by Hughes (1987) and Cook et al. (1989). Of the many texts on shells, Calladine (1983) places the most emphasis on basic physical understanding. Highly recommended is the guidance in detailed modeling of real shell structures provided by Bushnell (1974). Leissa (1973) collects all available results, computational and experimental, for the vibration of shells. Soedel (1994) provides a text devoted to shell vibration, containing many significant equations and results. Perhaps the most extensive collection of formulas for shells, including statics, dynamics, and stability, is given by Pilkey (1994).

Although shell structures cause difficulties for analysis, remember that they are also structures of marvelous beauty and high efficiency. In many applications, for example large domed stadiums, pressure vessels of all sizes, and hydrospace/aerospace vehicles, there is no other form to use because of the efficiency. So, let us deal with them.

CHARACTERISTICS OF SHELL RESPONSE

With all the complexity of a shell structure, there are a few crucial parameters that delineate the static and dynamic response of a shell segment. It is absolutely essential that the user of any code or method has some idea of what the correct response is. This is possibly more of a requirement for shells than with other structures, because the response of displacement and stress can differ by orders of magnitude, depending on the geometry and constraints. We attempt to provide a broad understanding by classifying the solutions in the following categories.

Extensional State

The *extensional* state, or *membrane* state, corresponds to stress and deformation for which the average stress across the wall is dominant, while the bending stress in the wall is relatively small. The prototype for this state is a balloon inflated with air, or the pressure can be external, as in an underwater vehicle. (Compressive stress, of course, causes the possibility of instability.) The key feature of the extensional state is that the deformation and stress vary smoothly and *slowly* along the shell surface. A slowly varying distribution is one that changes significantly in a distance, say, greater than one-eighth of the radius of the curvature of the surface. When the boundary conditions and loading are such that the extensional behavior dominates, the shell is very efficient in load carrying. The characteristic parameters, obtained from the axisymmetric behavior of a ring, are the magnitude of stress σ_E, displacement w_E, and the extensional frequency (in Hz) f_E:

$$\sigma_E = pR/t \tag{1}$$

$$w_E = pR^2/Et \tag{2}$$

$$f_E = \frac{1}{2\pi R}\left(\frac{E}{\rho}\right)^{1/2} \tag{3}$$

in which p is the magnitude of surface load, E is Young's modulus, ρ is the density, t is the thickness, and R is the radius of curvature of the boundary. More exactly, $1/R$ is the dot product of the curvature vector of the boundary curve and the unit normal to the surface. Whether a complete shell of revolution or a smooth shell

segment such as a panel, whether the shell consists of an isotropic or anisotropic composite material, these magnitude estimates are useful and can be made with local or averaged values of load, modulus, density, thickness, and radius of curvature.

Inextensional State

The *inextensional* state is opposite to the membrane state, corresponding to a deformation for which the bending stress in the wall is dominant, while the average stress across the wall, i.e., the extension of the wall, is small. An example for this state is a sheet of paper initially flat and then rolled into the shape of a cone or cylinder. A substantial change in the curvature of the surface takes place, while the extension of the surface is entirely negligible. The significant strain energy is due to the bending stress associated with the change of curvature. Like the extensional state, this state is also slowly varying. When the boundary conditions and loading are such that the inextensional solution dominates, the structural efficiency of the shell is very poor. However, if flexibility is desired, as in rolling the sheet of paper, so that large displacements are gained for little load, then the inextensional is the preferred state. The parameters, obtained from the nonsymmetric behavior of a ring, are the typical magnitude of stress σ_I, displacement w_I, and the inextensional frequency f_I:

$$\sigma_I = pR^2/t^2 \tag{4}$$

$$w_I = 3pR^4/Et^3 \tag{5}$$

$$f_I = f_E \frac{t}{R}. \tag{6}$$

To compare this with the extensional state, consider a shell with $R/t = 100$. The stress is two orders of magnitude larger, the displacement four orders of magnitude larger, and the first resonance frequency two orders of magnitude smaller. As seen by this comparison, for structural purposes the main design objective is to reinforce the shell properly to restrict the inextensional state, so that the primary state is extensional, (1)–(3), rather than inextensional, (4)–(6). Generally, this means that the shell needs stiffeners on the edges and at intersections of different shell segments.

Edge Bending State

The *edge bending* state is significant in a zone near the boundary. The width of this boundary zone, which we refer to as the *decay distance measure*, δ_{EB}, is called the characteristic length by MacNeal (1994):

$$\delta_{EB} = (Rt)^{1/2}. \tag{7}$$

Because the stress and deformation of this state change significantly in the relatively small decay distance, this type of solution is referred to as *rapidly varying*. For this state, both the average and bending stress in the wall are significant. The decay distance parameter is critical in the design of shells. For example, the rule of thumb for nozzles and openings is that reinforcement should be concentrated within the decay distance, where it is needed. When more than one nozzle is present, they should be spaced greater than δ_{EB}, to prevent significant interaction of the stress fields. When an opening or crack in the shell is smaller than δ_{EB}, the local self-equilibrating stress can be approximated by flat plate analysis.

Generally, when a shell is properly stiffened, the load is supported throughout the main portion of the shell by the extensional state. However, peaks in stress occur at boundaries and stiffeners, due to a combination of the extensional and edge bending states. The peak stress causes the initiation of cracks and local plastic flow. For static and low cycle loading of a shell made of a ductile material, the local plastic yielding causes an alleviation of the peak stress. Therefore, in conventional pressure vessel analysis the membrane stress is considered as "primary," and the edge bending as "secondary." However, in some cases the edge bending stress is much larger than the extensional and will not be alleviated with a little plastic flow. Generally, for high cycle vibration loading, the edge bending stress is of great significance. Inadequate analysis of this will cost in failure or the need for increased inspection and maintenance.

Edge Transverse Shear State

The *edge shear* state is even more localized, to a zone near the boundary of width equal to the shell wall thickness. This edge effect does not occur in the equations of classical plate and shell

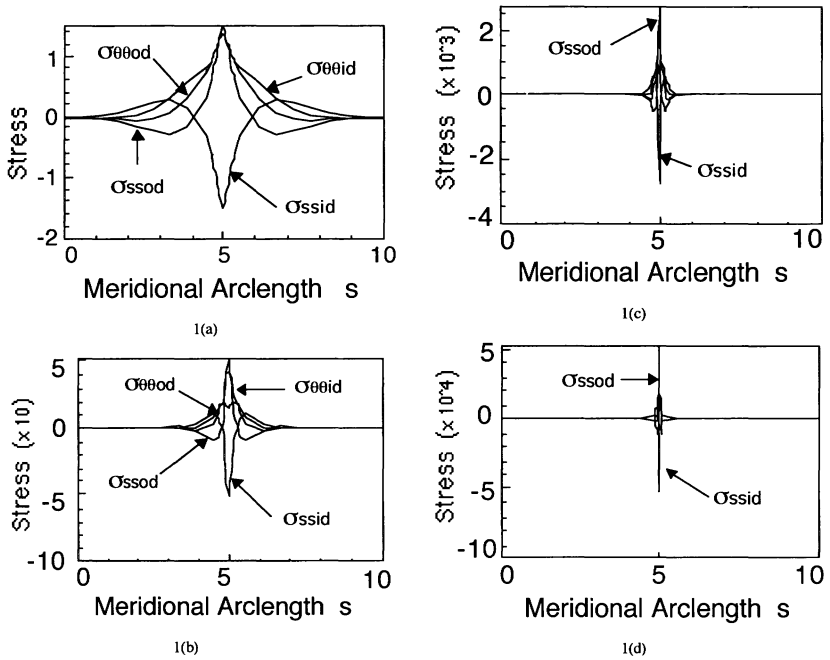

FIGURE 1 The effect of shell thickness on localization. This shows results for the distribution in the axial direction of the stress components in a cylindrical shell with free ends and axisymmetric ring load at the center. Except for the thickness, the parameters for each case are the same (steel, $R = 2$ m, $L = 10$ m, $f = 5$ Hz, $n = 0$). The radius-to-thickness ratio R/t is (a) 2, (b) 20, (c) 200, and (d) 2000. Local detail requires a very fine mesh for very thin shells.

theory. In the Reissner–Mindlin theory, sometimes referred to as a thick shell theory, transverse shear deformation is included that produces this additional edge state. Composites usually have a relatively soft matrix, so it is more necessary to include the transverse shear deformation. Indeed, to deal with composites properly, there are many higher order theories in use and being proposed on a daily basis. Particularly in the vicinity of a free edge, a layered composite requires essentially a three-dimensional solution. In addition, for either a composite or a homogeneous shell, material nonlinearity often occurs first in the shear layer and remains localized until failure.

Examples for Vibration

All four types of solutions are generally present to some degree, and in some problems, such as the cylindrical shell with a nozzle, are difficult to unscramble. However, only the edge bending state is present in Fig. 1, which shows the stress in a cylindrical shell with a uniform circumferential ring line load at the middle. This is the exact solution of the shell equations with transverse shear deformation included. The purpose of this figure is to emphasize that the localization becomes severe as the shell becomes thin. Figure 2 isolates the local shear layer. For this, at the center line the displacement and the meridional rotation are constrained while an external unit twisting moment is prescribed. The stress decays in about one shell thickness for the homogeneous shell. For a composite or sandwich shell for which the core or matrix is relatively soft, the shear layer will extend much further away from the edge.

Figure 3 shows the response of a cylindrical shell with a ring load at the center and free ends. However, instead of axisymmetric as in Fig. 1(c), the ring load varies around the circumference with $\cos 4\theta$, where θ is the circumferential angle. This is the term $n = 4$ in a general Fourier decomposition possible for a shell of revolution. For this situation, the inextensional state is not restricted and the frequency of excitation is above f_I. The result is a combination of all states. The slowly and rapidly varying parts can be clearly seen in the stress distribution Fig. 3(b). A conical

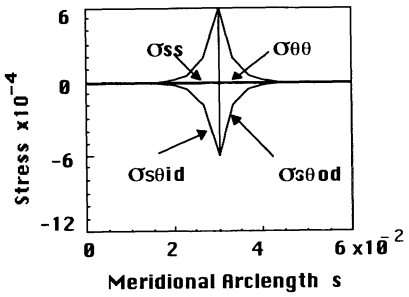

FIGURE 2 Local shear layer. This is for the same shell as in Fig. 1(c) (steel, R = 2 m, L = 10 m, f = 5 Hz, n = 2) showing the region of axial distance equal to three thicknesses on each side of the center. At the center, a unit twisting moment is prescribed, with the center displacement and the meridional rotation all constrained. The shear stress ($\sigma_s\theta$) is dominate for this loading and decays within one thickness.

shell is shown in Fig. 4 for low frequency excitation. With free ends for cos 2θ (n = 2), the deformation is almost purely inextensional. Even in the stress, Fig. 4(b), only a small effect of the edge bending state is apparent at the central line load and at the free ends. In contrast, Fig. 5 shows the same problem but with clamped ends. The peak stress is reduced by one order of magnitude with the clamping. The rapid and slow components are clear in the stress distribution in Fig. 5(b).

For a higher frequency, above the extensional frequency f_E, a typical displacement is shown in Fig. 6. In this frequency range the "edge bend-

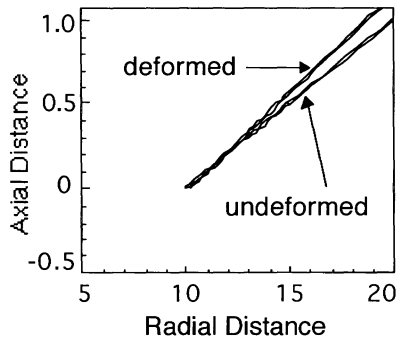

4(a)

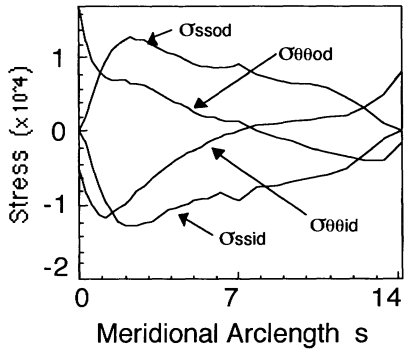

4(b)

FIGURE 4 Conical shell 45° with free ends with a ring load at the center, oscillating at a frequency f = 5 Hz, near the inextensional ring frequency of the larger end f_I = 3.4 Hz (n = 2, f_E = 438 Hz, R/t = 200). More than for the cylinder in Fig. 2, no effect of the localized load is seen in the deformation (a) and only a little in the stress (b). A computation with a course mesh can easily capture this behavior.

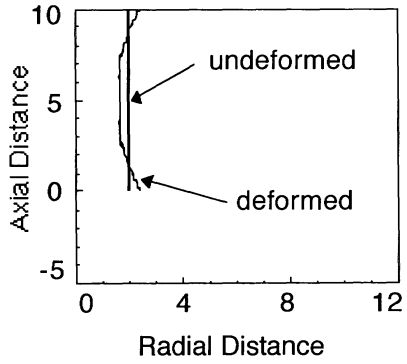

3(a)

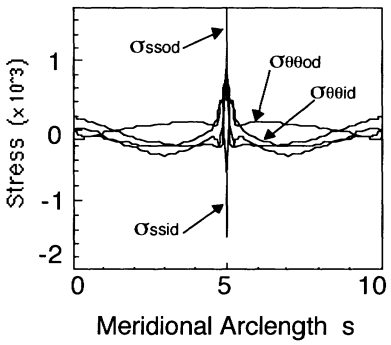

3(b)

FIGURE 3 Effect of excitation frequency f = 50 Hz, above the ring inextensional frequency (f_I = 4 Hz) for free ends. The deformed meridian is shown in (a) and the stress in (b). This is the same shell as in Fig. 1(c) (steel, R/t = 200, L/R = 10), but for harmonic of circumferential variation in the ring load n = 4. The lack of end constraint permits the nearly inextensional deformation that varies slowly along the meridian. The local effect in Fig. 1(c) is still present, strongly in the stress and less so in the displacement.

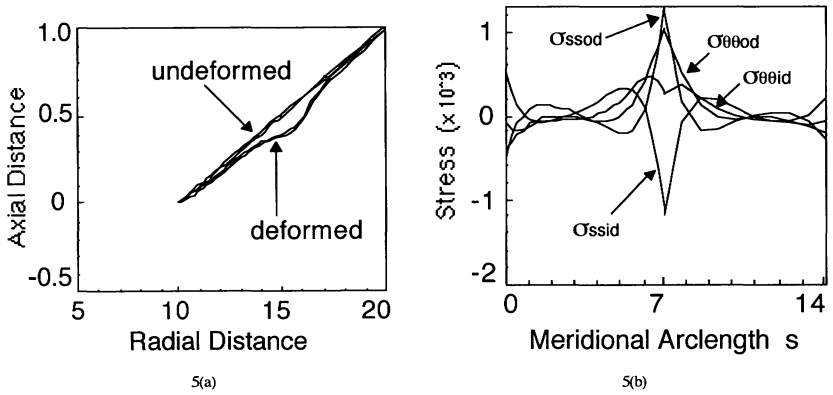

FIGURE 5 Conical shell 45° as in Fig. 4, but with clamped ends (n = 2, f = 5 Hz, f_E = 438 Hz, f_I = 3.4 Hz, R/t = 200). The end constraint greatly restricts the nearly inextensional component of deformation that reduces the total deformation (a) and the stress (b). The response is a combination of the slowly varying membrane behavior and the localized bending.

ing" changes to waves throughout the shell with a spatial wavelength on the order of magnitude of the decay distance δ_{EB}. The important point is that the "decay distance" in static problems becomes the wavelength in dynamic response for frequencies above f_E. An additional very important significance of f_E can be seen in Fig. 7. This shows the dispersion relation for the cylindrical shell in Fig. 1(c). If this cylindrical shell has length L = 5 m and simply supported ends, then the resonant frequencies occur near integer values of the dimensionless wave number k^*R. The lower branch of the dispersion relation in Fig. 7 starts with a steep slope, then abruptly flattens near the frequency f_E. Consequently many resonant frequencies occur slightly above f_E. This is similar for all the low circumferential harmonics and for any type of boundary conditions on any shell segment. For the particular cylinder in Fig. 6, there are around 100 resonances near f_E. Thus the typical thin shell is similar to a complex frame struc-

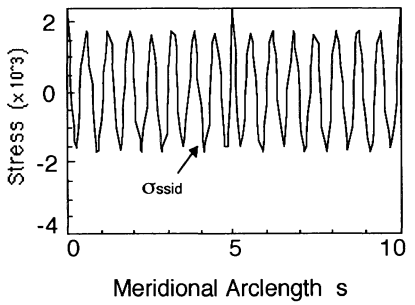

FIGURE 6 Distribution of stress component for excitation frequency f = 500 Hz, a little above the ring extensional frequency (f_E = 438 Hz). This is the same shell as in Fig. 1(c), (steel, R/t = 200, L/R = 10, clamped ends), but for the harmonic of circumferential variation in the ring load n = 2. The significant wavelength is the same order as the static decay distance in Fig. 1(c) for this and the many modes with frequencies near f_E.

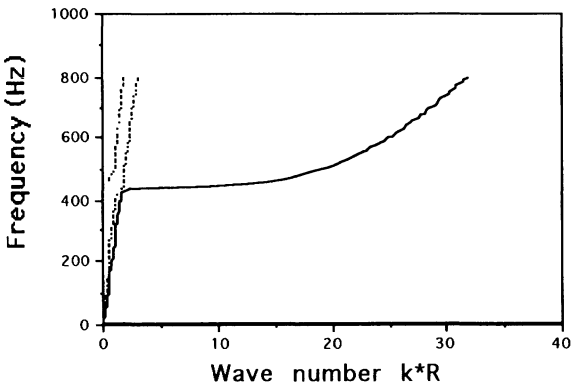

FIGURE 7 Dispersion relation for cylindrical shell (steel, R = 2 m, t = 0.01 m, n = 0). The resonances are at discrete values of the dimensionless wave number k^*R. For a length L = 10 and simply supported ends, these are close to every integer value of k^*R. The abrupt kink in the lower branch occurs near the ring extensional frequency f_E. Slightly above this there are around 10 resonances, or eigenfrequencies, at close to the same value that correspond to mode shapes similar to that in Fig. 4, i.e., with short wavelength. The higher branches give a number of resonances at high frequencies that correspond to long wavelength axial and shear modes. Each of the low circumferential harmonics has a similar behavior. In total there are around 100 eigenfrequencies close to the ring extensional frequency.

ture, in which many of the substructure units have resonances at nearly the same frequency. This must be anticipated when using modal decomposition techniques. To put it bluntly, modal decomposition is not useful in this frequency range.

For transient excitation, the speed of energy propagation is important. This is the group velocity, given by the slope of the curve in Fig. 7. Two branches are steep and correspond to extensional and shear waves. These have low wave number, i.e., long wavelength, so they are slowly varying, but travel very fast. Typically these are important on the microsecond scale of time. The lower branch in Fig. 7 gives waves with short wave lengths, on the order of magnitude of δ_{EB}. These waves travel slowly, and are important on a longer time scale, typically milliseconds.

Joining Shell Segments

In a typical shell structure there are many shell segments. A common approximation is to join the segments on the respective reference surfaces as indicated in Fig. 8(a). This is appealing because the shell equations reduce all variables to quantities defined on the reference surface. However, when the shell thickness is shown, as in Fig. 8(a), the approximation appears questionable because there is a gap on one side of the intersection and overlapping material on the other. When the slope of the two surfaces has a discontinuity as in Fig. 8(a), there is a further problem with the Reissner shell theory because the twisting moment vector has a discontinuity in direction. One way to balance this is to introduce the drill moment at the shell edge. This has been controversial (MacNeal, 1994), and informal reports indicate poor results when it is included in a shell element. A preferable treatment consists of a model with a ring at the intersection as indicated in Fig. 8(b) or for the intersection of several shell segments in Fig. 8(c). The ring or beam can support all three components of moment and force, so there is no inconsistency in equilibrium nor in the kinematics. Including transverse shear deformation in orthogonal directions of the ring cross section is exactly consistent with including transverse shear deformation in the plates and shells at the intersection. Furthermore this yields reasonable results for the case of the shell segments having substantially different thicknesses. Such a ring is used for the static nozzle intersection problem by Steele and Steele (1983). In subsequent work, excellent agreement was found between the shell calculation and three-dimensional photoelastic results when such a ring is used. To tie shell segments together only at the reference surface as in Fig. 8(a), it may be better to set the twisting moment equal to zero at the intersection rather than introduce the drill moment. The error will most likely only be in the small edge shear layer shown in Fig. 2. MacNeal (1994) recommends using solid elements in the vicinity of intersections. For modeling full details of fillets and weld seams, this is necessary. We are suggesting, however, that considerable accuracy can be gained with the ring element at virtually no cost in complexity. As pointed out by Schweizerhof et al. (1992), three-dimensional elements have the disadvantage of introducing many high frequency, through-thickness modes of response that require a very fine time step in an explicit calculation of the dynamic response. The through-thickness modes would appear in Fig. 7 as additional high frequency branches.

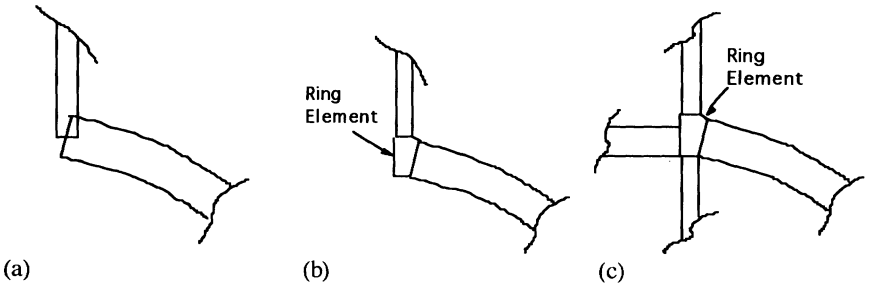

FIGURE 8 Joining shell segments. Often plates and shells are joined at the meridian as in (a). However, this is physically inconsistent and causes the concern for the drilling degree of freedom at the intersection. Introducing a ring or beam element at the intersection of two shells (b) or more shells (c), is easy, physically reasonable, avoids any need for consideration of the drill, and yields much better agreement with the experiment.

COMPUTATION

The physical behavior just described provides a substantial challenge for numerical computation. Equations that have rapidly varying solutions, either in boundary layers or in waves, are referred to as "stiff." For stiff systems, most popular methods of numerical analysis are not applicable. Direct application of forward integration in the spatial coordinates with "shooting" is not practical. Similarly, the transfer matrix method that is useful for some problems such as beam frameworks, can be used only for short, thick shells. Also, the boundary element method, which is very useful for many problems in mechanics, has found only restricted application for shells. The main drawback is that simple, fundamental point load solutions for a general surface are not available. In much of the literature on the numerical analysis of stiff systems, restrictive assumptions are invoked that exclude most significant shell problems, such as in Kreis (1992). Thus the most widely used approach is with finite elements in a spatially implicit formulation. However, as discussed by MacNeal (1994), the search for the ideal shell element continues. Rather than consider the details of element architecture and the various difficulties, which is well documented in the references, we focus on the general problems of modeling shell response with any spatially implicit, discrete method.

Mesh Spacing

A criticism of most commercial codes is that the important matter of mesh generation is entirely left to user judgment. The situation is improving with current research codes having the capability for automated, adaptive mesh refinement. Additionally, the *p*-element codes provide automatic error checking and enhancement of the shape functions within the element. The indication is that these techniques are being implemented in the general commercial codes. In the meantime, some of the current mesh generators produce mesh size that is "small," "medium," or "large," at the users discretion, without much hint of the consequences of such a selection. Of course, a good check on the validity of the solution is to rerun with double the number of elements. For a complex shell structure, it is often the case that such a mesh refinement study is not practical. So, let us consider the sort of mesh necessary to get a good solution the first time. Consider the mesh required to capture the localization shown in Fig. 1 for low frequency and the short wavelength for high frequency shown in Fig. 6. Generally, at least four low order finite elements are needed in the decay distance δ_{EB}. For *p*-element refinement, the shape functions are enhanced by higher order polynomials within the element. However, the polynomials become unstable when fitting strong exponential or oscillatory behavior, so there is a limit to the order of the polynomial. This limits the size of the *p* element to, say, one decay distance δ_{EB}. The *p* elements are not as versatile for nonlinear behavior, however, so we consider only the low order element. For a uniform mesh of square elements, four per decay distance, the total number of elements N_{EB} needed to capture the edge bending is then:

$$N_{EB} = \frac{2\pi RL}{Rt/16} = \frac{32\pi L}{t}. \tag{8}$$

To capture the transverse shear edge zone the number of elements is N_{ES}, given by:

$$N_{ES} = \frac{2\pi RL}{t^2}. \tag{9}$$

For the dimensions of the shell in Fig. 1, the values of N_{ES} and N_{EB} are shown in Table 1. For the thin shell the number of elements is large. Because a typical shell structure consists of many such shell components—spheres, cylinders, cones, rings, stiffeners—using a mesh to meet (8), not to mention (9), in the entire structure is generally not practical.

What is the consequence of not meeting (8) and (9)? There does not seem to be a clear answer to this. However, there are many examples for the static and low frequency response range, with frequency less than f_E (3), that show that only the edge effects are lost. Thus an important and

Table 1. Number of Square Elements in Uniform Mesh Needed to Capture Edge Effects in Cylinder with $L/R = 5$

R/t	N_{EB} for Edge Bending	N_{ES} for Edge Shear
20	10^4	10^4
200	10^5	10^6
2000	10^6	10^8

comforting fact is that correct results are obtained for the slowly varying extensional and inextensional solutions. Of course, for local loading, such as the line load in Figs. 1–3 and 5, the main part of the solution, the peak stress, is lost when the mesh is too coarse. For the shell with unrestrained ends, for which the purely inextensional deformation is possible such as in Fig. 4, the main part of the solution is inextensional. The deformation of the meridian Fig. 5(a) consists of almost a rigid rotation. This is easily captured with a coarse mesh. In the stress Fig. 5(b), all that is lost with a coarse mesh is the little bump in the middle under the load and the details at the ends. However for distributed loading, such as pressure, acting on a shell with proper stiffening to restrain the inextensional solution, the extensional state is the main component of the solution. All that is lost is the edge region of bending, that typically gives a stress concentration around 2–3.

So, *be aware*. Most finite element calculations of shells we have examined miss peak stress by this factor of around 2. A special effort must be made to get the peak stress. Also be aware that at unreinforced slope discontinuities in shells, such as the intersection of a cone and a cylinder or a nozzle in a cylinder, a coarse mesh can miss the peak stress by a factor of as much as 10. A basic problem with finite elements is that the edge stress is obtained by extrapolation from interior values, which tends to undershoot the edge value in regions of exponential variation. It can be added that this is also a problem with experimental strain gage measurements of thin shells. It is difficult to get a gage close enough to the intersection to catch the peak stress.

For the low frequency range, frequency less than f_E (3), the correct resolution is reasonable and practical. Use a variable mesh spacing, with a coarse mesh in the main part of the shell component graded to a fine mesh near regions of discontinuity of load and geometry. For a distance of at least $3 \times \delta_{EB}$ near the boundary of discontinuity pack in, say, 12 elements. To capture the edge transverse shear, a finer mesh should be used, consisting of, say, at least four elements within a distance of two thicknesses. Do the calculation of δ_{EB}, and do not depend on what looks like a reasonably fine mesh. For a thin shell, what appears to be sufficiently fine may not be at all. A coarse mesh will give a smooth result for the distribution of stress and displacement. This is *not* necessarily an indication that the results are valid.

If peak stress is not important, and only the overall response of a shell structure in the low frequency range is desired, such as for a launch vehicle, then a coarse mesh is probably adequate. Popular validation problems for finite elements (MacNeal, 1994) are the pinched hemisphere, the pinched cylinder, and the Scordelis–Lo roof. These are all problems with free edges in which the inextensional state (or nearly inextensional in the Scordelis–Lo roof) dominates. Thus a coarse mesh can capture the deformation. The stress, which requires a finer mesh, is often not considered in validation problems. However, the problems with dominant inextensional state are nontrivial test problems, because the boundary conditions at a free edge are nearly singular for a thin shell. Users should be aware that a mesh that just passes these tests will not be adequate for the important local effects.

The mesh requirement for a thin shell is a formidable obstacle for finite elements. Consequently there is ongoing research on alternate approaches, which might be classified as "large element" approaches. In these a complete set of exact solutions are used, so that one element can contain multiple cracks and holes. Excellent results for plates and two-dimensional elasticity have been obtained by the hybrid-Trefftz method of Jirousek (1987), and the edge function method of Quinlan (1987). A glance at the localization for a thin shell in Fig. 1 suggests that a combination of asymptotic analysis and the edge function method should be applicable for shells. A beginning is represented by the FAST2 program of Steele and Steele (1983), in which a large, thin cylindrical shell with a hole is treated as one "element." Work is in progress toward generalizing the approach. As pointed out by Kreiss (1992), after all the analytical effort that has been expended on asymptotic analysis of such systems of equations, it is surprising that little of this analysis has been converted into efficient numerical methods.

Modal Analysis

Once the stiffness, damping, and mass matrices are determined for a shell structure from the finite element or other formulation, the modal method provides a convenient means for determining the response in the frequency or time domain. In standard modal analysis the displacement and forcing functions are expressed as a sum of the eigenvectors of the corresponding eigenproblem. When the damping matrix is written in an orthogonal

form such as for Raleigh damping, the orthogonality property of the eigenvectors can be used to uncoupled the equations of motion. A solution is then found for each eigenmode either exactly or numerically. The modal solutions are then superposed to reconstruct the total structural response. For any continuum, the solution is approximate because a truncation must be made in the number of modes used. The accuracy of the approximation is dependent on how well the modes selected can represent the forcing and displacement.

For excitation of a complex shell structure in the low frequency range, $f < f_E$ for each component, this standard modal approach is generally successful. Particularly when only the global response characteristics are desired, the local effects are ignored and a coarse mesh used. The helicopter is a good example of a complex structure for which the dynamic response is crucial. In a fairly recent model the first production helicopter had the frequency of the torsional mode of the tail at exactly the blade strike frequency. To avoid such occurrences, several companies joined in an effort to improve and document the use of NASTRAN as a predictive tool in design, as reported by Kvaternik (1993). The results show that the first few resonances can be predicted. All the simulations must be considered as "coarse," modeling the shell structure as rings and stiffeners connectd by shear panels and assuming a fixed 2% modal damping. However, after the first few modes, the agreement with the experimentally determined response is not satisfactory. Improvement may come with better modeling of the curved panels as shells and with better identification and modeling of the damping. It appears that the use of composites will increase, corresponding to larger panels that carry a larger portion of the load. Therefore the need for accurate shell capability will increase. Another study involving many companies is reported by Kielb et al. (1985). In this the resonant frequencies of a twisted plate were considered, because this is of fundamental concern in the design of turbomachinery blades. The frequencies were computed independently by a number of finite element codes, and the results compared with an experiment and an exact calculation. Although some of the best-known computational procedures were used by analyists with great experience, the numerical results obtained showed considerable disagreement. Some even showed the incorrect trend of frequency change with increasing angle of twist for the first mode. Use of large numbers of elements did not necessarily lead to accurate results. We presume that the codes by the present time have been improved to give the correct behavior on this particular problem. However, careful validation remains important.

For the high frequency range of response, $f > f_E$ for some components, the modal approach encounters difficulties for shell structures. The first resonant mode for each shell may look like that in Fig. 7. Thus the fine mesh with the number of elements N_{EB} in Table 1 is necessary for each component. Calculation of the eigenvalues and corresponding eigenvectors is expensive for such a large system. Second, the number of resonances near the extensional frequency f_E can be large. There is a major problem in identifying all these eigenvalues. Furthermore, methods designed for systems with discrete eigenvalues, with perhaps the provision for handling two or three repeated eigenvalues, may not be appropriate when, say, 100 eigenvalues are in close proximity. Generally, for thin shell structures, different components have different values of f_E, so several clusters of resonant frequencies are present. For these reasons, the modal approach is limited in dealing with high frequency response.

Direct Integration Methods

Following is a brief outline of the basic features of direct integration methods. The time derivatives in the equation of motion are replaced by finite difference approximations. The nature of the difference equations can be grouped as either explicit or implicit in time. In the explicit scheme the current solution is described exclusively in terms of past values. In the implicit scheme the solution is expressed in terms of past and current values. The difference equations reduce the problem to the solution of a system similar to the static case at each time step. Thus these methods are readily adaptd to nonlinear problems.

Explicit methods in general have the property that when diagonal mass and damping matrices are used the system of equations to be solved uncouple and can be advanced in time directly, without the computational cost of solving a simultaneous system. However, this advantage may be offset by the limitation imposed by conditional stability. A commonly used explicit algorithm is the central difference method. It is conditionally stable and second-order accurate. For the central difference method, stability requires that the time step be less than twice the inverse of the highest

natural frequency of the system. Because too small a time step increases the cost of the time history analysis, it is important to have a good estimate of the maximum frequency present. If an eigenvalue calculation is not available, then an upper bound on the maximum frequency can be found by calculating the highest natural frequency of a constituent element.

Explicit schemes are most efficient when high frequency components are of critical interest, such as is typical of impact and wave propagation problems. The computational simplicity of advancing the solution in time makes the cost per time step small. However, explicit methods may be impractical when a long time history is required.

Implicit schemes may be better suited to the large time solution requirements because they can be unconditionally stable. Some examples of implicit algorithms in use are the trapezoid rule, Houbolt method, Park method, α method, and the Wilson-θ method. These share the properties of unconditional stability and second-order accuracy. Excluding the trapezoidal rule, these methods also contain numerical damping that can be useful in removing the contribution from undesired high modes that may be spurious relics of the discretization process.

The time step used in these implicit schemes is limited by the desired solution accuracy. Typically, at least 10–20 time steps per period of the highest desired mode are required to accurately capture that mode. Solutions at large times may be dominated by a few low frequencies only. In this case large time steps that are orders of magnitude greater than possible in the explicit schemes may be used to quickly bring the solution to equilibrium. While the per time step computations are expensive due to the necessity of solving a large system of equations, the unconditionally stable behavior may make the implicit method more efficient for problems where only a small number of modes contribute to the solution at a desired instant in time.

One aspect of the computational difficulty of shells, compared with solids and plates, is apparent in Fig. 7. The lower branch is important for the long-time response and requires a fine mesh. The higher two branches correspond to slowly varying waves that can be captured with a coarse mesh, but have a high speed of energy propagation, on the order of magnitude of the compression and shear waves in a solid. Very small time steps are required in an explicit solution to capture the fast waves. However, a fine mesh is required to capture the short wavelength modes given by the lower branch, which have a very significant effect at long times. Thus for the shell we have the double demand for a fine mesh over the entire surface and very short time steps. For the implicit scheme, the larger time steps permit the computation of the longer time response, at a loss of the short-time detail. However, it is typically the case, that the significant deformation and stress occurs at the longer time scale at which the short wavelengths are significant. Thus the fine mesh is still required.

Examples

The experienced analyst can reduce the number of elements required in a particular case. Figure 9 is taken from Prantil et al. (1986), and shows the permanent deformation resulting from explosive loading of a cylindrical shell. The loading occurred in 80 μs, while the maximum strain measured in experiment occurred at around 1 ms, in correspondence to the previous discussion on resonant frequencies. The calculation was performed with DYNA3D, using a modified Hughes–Lu shell element. The R/t ratio was selected so the response would have significant elastic and plastic effects. For thinner shells elastic effects dominate, and for thicker shells plastic

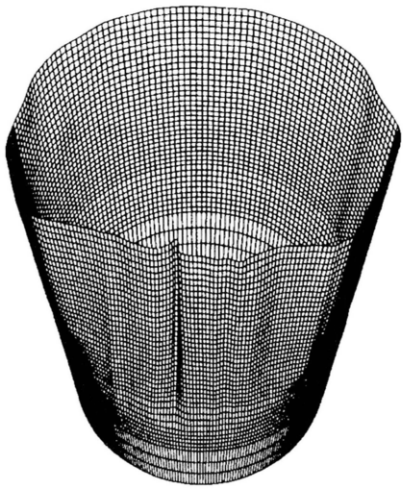

FIGURE 9 Final form of a cylindrical shell subject to blast loading. An explosive pad was distributed on half of the shell length and half of the circumference ($R/t = 270$, $L/R = 3.4$). A distribution of imperfection was assumed that produced good qualitative agreement with the final deformation in the experiment, using 10,080 elements in DYNA3D. Adapted from Prantil et al. (1986).

flow is most significant. According to (8), this shell requires 90,700 uniform and square elements. In fact 10,080 were used to obtain good qualitative agreement with the experimental results. These elements were not uniform but concentrated in the central portion of the shell. Furthermore the elements were selected to have twice the length in the axial direction as in the circumferential. As seen in Fig. 9, the sharp spatial variation occurs in the circumferential direction. Thus with knowledge of the significant deformation pattern for a specific loading, the number of elements can be reduced from the estimate (8), while retaining good results. It should be noted, however, that the laboratory (SRI) had 30 years of experience in the analysis and computation of this problem, and the developer of the code (Hallquist, 1994) assisted in this computation. Even with the advances in the last few years, good results for such problems are not to be considered routine. Finally note in the title that the shell is considered as very thin, with $R/t = 267$. In fact many liquid storage vessels, rocket motor cases, and reactor containment vessels are in the range $R/t = 1000$–4000. From Table 1, the number of elements for such shells becomes large indeed. In other types of explosive loading of the shell, full resolution in the axial direction is required. In Fig. 10 is the response for a step load moving along a beam on an elastic foundation. The behavior is similar to that of a shell of revolution with a step pressure, say a shock wave in air, moving along the shell in the axial direction. The stiffness of the elastic foundation varies. In Fig. 10(a), the load is moving to the stiffer end, corresponding to a wave moving from the big end of a conical shell toward the smaller; in Fig. 10(b) the load moves in the opposite direction. The correct solution requires the capture of the waves moving ahead of the load, which have the wavelength on the order of magnitude of δ_{EB}.

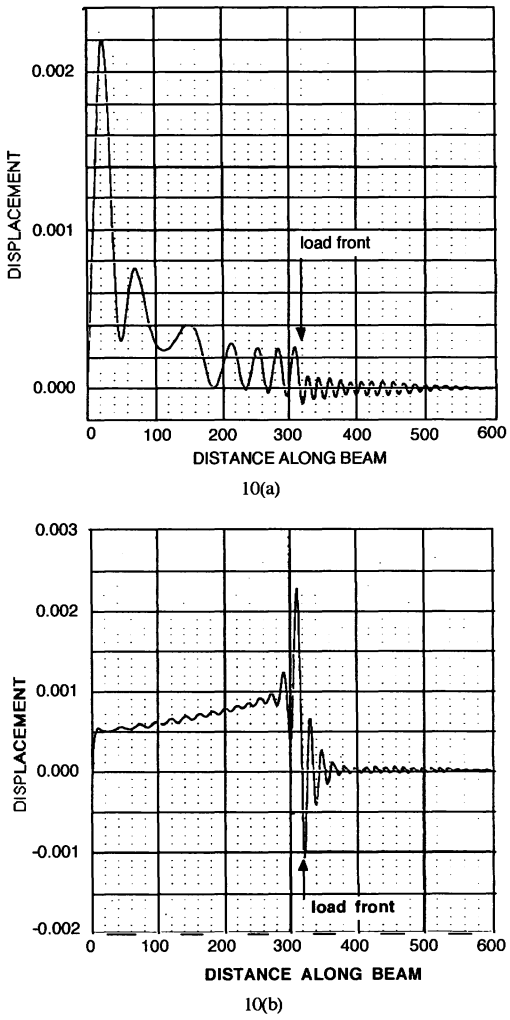

FIGURE 10 Step pressure load moving along a beam on an elastic foundation of varying foundation modulus. This is the behavior of a conical shell subject to a blast wave in the surrounding air traveling along the axis. In (a) the load is moving from the soft to the stiff region, i.e., from the big end to the small end of the cone; in (b) the load is moving from the stiff to the soft region. (Computations from P. Underwood.)

In the large deformation of thin shells, just as in crumpling a sheet of paper (or in Fig. 9), the deformation pattern can be recognized as consisting of regions in which the inextensional state dominates connected by narrow ridges in which the edge bending state dominates. A simple example of this is in Fig. 11(a) that shows the impact of a thin spherical shell against a rigid wall. In Fig. 11(b) the spherical shell is impacted by a small mass. In both cases, an inverted dimple forms. The Gaussian curvature of the dimple is the same as before, because changing the Gaussian curvature requires a high amount of extensional state energy. The outer region and the inverted dimple region are connected by a narrow region of high bending stress. The significant strain energy and/or plastic flow occurs in the narrow region. Thus a fine mesh is needed to capture this behavior. However, the location of the rim is changing as the dimple increases in size, so either an adoptive mesh technique or a fine mesh everywhere is required. For thicker shells the narrow bending region is dominated by plastic flow. At first glance this would seem to be pure loading as the dimple progresses. However,

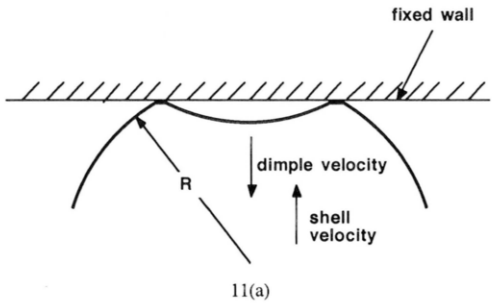

11(a)

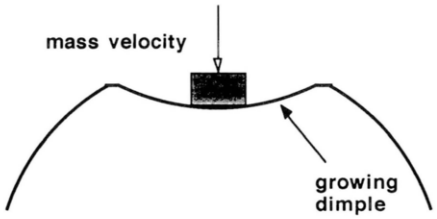

11(b)

FIGURE 11 Impact of shells. For large deformation of shells, the shell will generally have regions of inextensional bending divided by narrow regions of edge bending. In (a) a spherical shell impacts a rigid wall and in (b) a mass strikes a spherical shell. In both a dimple forms with the same curvature as the original shell. For elastic deformation, the significant strain energy is in the narrow transition region. When the elastic limit is exceeded, plastic flow occurs in the transition region. Note that a fixed point on the shell experiences plastic bending and then reversed bending, so unloading must be handled properly. As the dimple progresses further, asymmetric bifurcations in the deformation shape usually take place.

a point on the meridian initially has the radius of curvature R. As the bending region reaches the point, the radius of curvature decreases substantially, causing plastic flow. As the bending region passes the point, the bending of the point reverses direction and ends up with the negative radius of curvature $-R$. Thus significant unloading takes place, which must be taken into consideration for correct results. As the dimple progresses further, bifurcations of the bending region into asymmetric modes takes place.

Figure 12 shows the side impact of a cylindrical shell on a rigid plate, from Lovejoy and Whirley (1990). The regions of the nearly inextensional state and the narrow regions of the edge bending state can be seen, even for this fairly thick shell. For this computation, a uniform mesh of brick

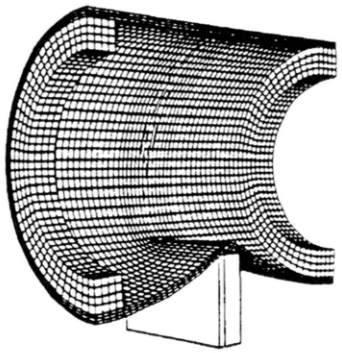

FIGURE 12 Impact of a cylindrical shell on a rigid plate with DYNA3D. Adapted from Lovejoy and Whirley (1990).

elements is used. Finally, a very challenging problem of the simulation of an automobile crash is shown in Fig. 13, taken from Hallquist (1994). Such a structure contains many solid, plate, and shell elements. Future lighter weight designs are moving in the direction of more thin shell-like components, so more of the thin shell difficulties discussed in this article will have to be met. The capability for complete analysis of such structures is being aggressively pursued by several automobile companies.

CLOSURE

The message has gotten across in many areas of industry that the gain in understanding through computation is far less expensive than extensive experimental studies, and far, far, less expensive than recalls and court settlements resulting from inadequate design. Nonetheless, there are reports from designers who seem to be under more pressure than ever. The high competition and shorter design cycle allows insufficient time for either proper experimental testing or computational simulation. However, we expect the increase in computer power and the sophistication of numerical simulation to continue unabated. We hope

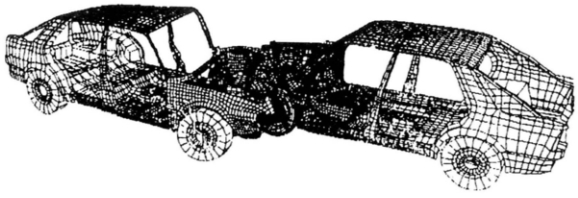

FIGURE 13 Automobile crash simulation with LS-DYNA3D. Adapted from Hallquist (1994).

that the points mentioned in this article will aid in a realistic understanding of the present and near future capability for the analysis of shell structures.

REFERENCES

Brebbia, C. A., Ed., 1985, *Finite Element Systems, A Handbook*, Springer, Berlin.

Bushnell, D., 1974, "Thin Shells," in W. Pilkey, K. Saczalski, and H. Schaeffer, *ONR/NSF Symposium on Structural Mechanics Computer Programs,* University Press of Virginia, Charlottesville.

Calladine, C. R., 1983, *Theory of Shell Structures*, Cambridge University Press, Cambridge, UK.

Cook, R. D., Malkus, D. S., and Plesha, M. E., 1989, *Concepts and Applications of Finite Element Analysis*, 3rd ed., Wiley, New York.

Hallquist, J. O., 1994, SU-DYNA3D Information Pamphlet.

Hughes, T. J. R., 1987, *The Finite Element Method*, Prentice–Hall, Englewood Cliffs, NJ.

Hughes, T. J. R., and Hinton, E., Eds., 1986, *Finite Element Methods for Plate and Shell Strucures*, 2 Vols., Pineridge Press, Swansea, UK.

Jirousek, J., 1987, "Hybrid-Trefftz Plate Bending Elements with *p*-Method Capabilities," *International Journal of Numerical Methods in Engineering*, Vol. 24, pp. 1367–1393.

Kardestuncer, H., Ed., 1987, *Finite Element Handbook*, McGraw–Hill, New York.

Kielb, R. E., Leissa, A. W., and MacBain, J. C., 1985, "Vibration of Twisted Cantilever Plates—A Comparison of Theoretical Results," *International Journal of Numerical Methods in Engineering,* Vol. 21, pp. 1365–1380.

Kreiss, H. O., 1992, "Problems with Different Time Scales," *Acta Numerica*, pp. 101–139.

Kvaternik, R. G., 1993, "A Government/Industry Summary of the Design Analysis Methods for Vibrations (DAMVIBS) Program," NASA Conference Publication 10114.

Leissa, A., 1973, *Vibration of Shells*, NASA SP-288.

Lovejoy, S. C., and Whirley, R. G., 1990, DYNA3D Example Problem Manual.

MacNeal, R. H., 1994, *Finite Elements: Their Design and Performance*, Marcel Decker, New York.

Noor, A. K., Belytschko, T., and Simo, J. C., 1989, *Analytical and Computational Models of Shells,* CED-Vol. 3, Amer. Soc. of Mech. Eng., New York.

Pilkey, W. D., 1994, *Formulas for Stress, Strain, and Structural Matrices*, Wiley–Interscience, New York.

Prantil, V. C., Kirkpatrick, S., Holmes, B. S., and Hallquist, J. O., 1986, "Response of a Very Thin Shell Under an Impulsive Radial Load," in T. J. R. Hughes and E. Hinton, Finite Element Methods for Plate and Shell Structures, Vol. 2: Formulations and Algorithms, Pineridge Press, Swansea, UK, pp. 252–262.

Quinlan, P. M., 1987, "The Edge Function Method for 2-D Fractures," in C. A. Brebbia, W. L. Wendland, and G. Kuhn, *Boundary Elements IX*. Springer-Verlag, Berlin.

Sanders, J. L., 1959, "An Improved First-Approximation Theory for Thin Shells," NASA Report 24.

Schweizerhof, K., Nilsson, L., and Hallquist, J. O., 1992, "Crashworthiness Analysis in the Automotive Industry," *International Journal of Computer Applications in Technology*, Vol. 5, Nos. 2/3/4.

Soedel, W., 1994, *Vibration of Shells and Plates*, 2nd ed., Marcel Dekker, New York.

Steele, C. R., and Steele, M. L., 1983, "Stress Analysis of Nozzles in Cylindrical Vessels with External Load," *Journal of Pressure Vessels and Piping*, Vol. 105, pp. 191–200. (See also Welding Research Council Bulletins WRC 297, 335, 337, 368.)